Ground state configurations and melting of two-dimensional non-uniformly charged classical clusters

2009 J. Phys.: Condens. Matter 21 155301

(http://iopscience.iop.org/0953-8984/21/15/155301)

J. Phys.: Condens. Matter **21** (2009) 155301 (7pp) doi:10.1088/0953-8984/21/15/155301

Ground state configurations and melting of two-dimensional non-uniformly charged classical clusters

D M Tomecka[1,4], G Kamieniarz[1,2], B Partoens[3] and F M Peeters[3]

[1] Institute of Physics, A Mickiewicz University, ulica Umultowska 85, 61-614 Poznań, Poland
[2] Max Planck Institute for the Physics of Complex Systems, Nötnitzer Strasse 38, D-01187 Dresden, Germany
[3] Department of Physics, University of Antwerp, Groenenborgerlaan 171, 2020 Antwerp, Belgium

E-mail: Daria.Tomecka@amu.edu.pl

Received 22 November 2008, in final form 23 February 2009
Published 17 March 2009
Online at stacks.iop.org/JPhysCM/21/155301

Abstract
We consider classical two-dimensional (2D) Coulomb clusters consisting of two species containing five particles with charge q_1 and five with charge q_2, respectively. Using Monte Carlo and molecular dynamics (MD) simulations, we investigated the ground state configurations as well as radial and angular displacements of particles as a function of temperature and their dependence on the ratio $q = q_2/q_1$. We found new configurations and a new multi-step melting behavior for q sufficiently different from the uniform charge limit $q = 1$.

(Some figures in this article are in colour only in the electronic version)

1. Introduction

Coulomb clusters, made out of point charged particles confined by a parabolic potential, are of general interest not only for classical but also for quantum systems. The ground state configuration and melting of such systems have been widely studied [1–8]. The model system of 2D confined clusters of classical particles, known also as a classical Wigner molecule, is the classical analog of the well known quantum dot problem [9]. It closely describes quantum dots in the weak density limit and/or in the high magnetic field limit [11, 12], where the kinetic energy of the electrons is quenched. In a finite system there is a competition between the bulk triangular lattice and the circular confinement potential that tries to force the particles into a ring-like configuration [13]. These quantum dots (called also artificial atoms) are atom-like structures that have interesting optical properties and may be of interest for single-electron devices [9], they can serve as hosts for storing quantum information, i.e. qubits, because of their atom-like properties [14]. When one increases the ratio between the average kinetic energy and the average potential energy the system will lose its order and it will melt. For the classical system this is done by increasing temperature or by decreasing the density, i.e. increasing the average distance between the particles. At $T = 0$ the classical system will always be in the ordered state. This is different from the quantum analog where one can increase the quantum fluctuations by increasing the density of the particles, resulting in quantum melting. This regime was studied in [10] using the path integral Monte Carlo (MC) method which was extended in [11] to non-zero temperatures.

The model system itself was introduced for the first time by Thomson [15] as a classical model for the atom, where a small number of electrons are placed in a uniform neutralizing ion background, generating the parabolic confining potential. For a small number of equally charged particles (up to $N = 50$) such systems form concentric shells [1–3, 9, 16]. For magic configurations these shells consist of a few subshells [8] with slightly different radii. The radial order in such shells is maintained until angular order between different shells is lost. In non-magic configurations, the fine structure in a shell is lost at very low temperatures while radial order persists up to much higher temperatures. In a very large system, the radial and the intrashell angular order of all the shells disappear at the same temperature.

In the present paper we investigate a binary system and study in detail how the inequality of the two types of particles

[4] Author to whom any correspondence should be addressed.

influences the ground and metastable states and the melting of the cluster. Because of the increased parameter space, we limit ourselves to a cluster consisting of ten particles with an equal number (i.e. five) of particles with two different charges. We find the ground state configurations for varying ratio $q = q_2/q_1$ and determine the new melting scenario in the region $0 \leqslant q \leqslant 5$ in the particular case $N_1 = N_2 = 5$.

Non-uniform systems of charged particles containing a small number of defects have been studied recently [5, 17, 18]. As to binary systems [12, 19], previous studies focused on the case of $N_1 \neq N_2$. Detailed MC simulations of the case $N = 13$ ($N_1 = 7, N_2 = 6$) show that the intrashell melting temperature $T_{\alpha 1}$ (figure 3 in [19]) is lower than the radial melting temperature T_{r} for the internal shell in the region $0.1 \leqslant q \leqslant 0.5$ and increases monotonically with q. For $q \approx 1$ (figures 10 and 11 in [19]) a similar behavior is revealed for the radial T_{r} and the angular intershell melting temperature $T_{\alpha 2}$. However, the q dependence is not monotonic. T_{r} reaches a maximum, while $T_{\alpha 2}$ a minimum for $q \to 1$. For $q = 3$ (figure 1 in [19]) the intershell melting temperature $T_{\alpha 2}$ is also the lowest one (corresponding to the mean square displacements equal to 0.1). The radial and intrashell melting temperature T_{r} and $T_{\alpha 1}$ for the internal shell are roughly the same.

In fact, this scenario holds for $q > 1.9$ (figure 2(b) in [19]). For both $N = 13$ and 25 and particles with equal masses, the radial melting temperature of inner shell(s) is lower than that for the outer shell (particles with a smaller charge melt first).

For the binary system consisting of 10 particles (with $N_1 = N_2$), a perfect ring-like structure was found in [12] (their figure 2(a)). It appears in the ground state for $q \leqslant 0.5$ and $q \geqslant 2.0$, while in the region $0.5 < q < 2.0$ there are deformations.

The non-uniform system with N_{s} particles carrying the charge $q_1 = 1$ and N_{d} carrying the charge $q_2 = 2$ has been analyzed by Drocco *et al* [5]. In this study the charges were fixed and the number of particles was changed. They found that the outer shell is formed by doubly charged particles and the highest melting temperature corresponds to $N_{\mathrm{s}} = N_{\mathrm{d}} + 1$.

In the present paper we extend previous work on finite size binary systems to a larger range of q-values; we also obtain the metastable states and investigate the different melting regimes. This paper is organized as follows. In section 2 we introduce the model system and the algorithm used. The numerical results on the ground and metastable states of the melting of our system are studied in section 3. Our results are also summarized in section 3.

2. The model and MD simulations

Our system consists of $N = 10$ non-equally charged particles, which interact through a repulsive Coulomb potential and move in two dimensions (2D). $N_1 = 5$ particles carry a charge q_1 and $N_2 = 5$ particles carry a charge q_2. We define $q_1 = 1$ and $q_2 = q = q_2/q_1$. The system is held together by the confining parabolic potential $V(r)$ and the total potential energy is given by

$$U = \sum_{i=1}^{N=10} \left(V(r_i) + \frac{q_i}{e} \sum_{j=i+1}^{N=10} \frac{q_j}{|r_i - r_j|} \right),$$

where $V(r) = \frac{1}{2} m {\omega_o}^2 r^2$.

The potential energy can be written in a reduced form (in dimensionless units) as

$$U = \sum_{i=1}^{N} \left({r_i}^2 + \sum_{j=i+1}^{N} \frac{q_i q_j}{|r_i - r_j|} \right), \tag{1}$$

where we introduced the notation [2]:

$$r_o = (2q_1q_2/\epsilon)^{1/3}\alpha^{-1/3}, \qquad E_o = (q_1q_2/2\epsilon)^{2/3}\alpha^{1/3},$$

$$T_o = (q_1q_2/2\epsilon)^{2/3}\alpha^{1/3}\, k_{\mathrm{B}}^{-1}, \qquad \text{with } \alpha = m{\omega_o}^2,$$

where ω_o is the vibration frequency of a single particle in the parabolic confinement potential, m is the mass of the particle, q is the relative particle charge and ϵ is the static dielectric constant of the medium in which the particles are moving.

The stable configurations of the particles in our systems are found by using a MC simulation technique applying the Metropolis algorithm [20] together with a Newtonian optimization technique (which improves the accuracy of the MC method). A more detailed description of it can be found in [3]. In that method the particles are initially thrown in random positions within some circular area (in the confining potential) and than allowed to reach a steady state configuration. To reach the ground state we use 10^3 MC steps during which all the particles are randomly displaced. If the new configuration has a smaller energy than the old configuration the displacement is accepted. If the new energy is larger than that corresponding to the old configuration the displacement is accepted with probability $\delta < \exp(-\Delta E/T)$, where δ is a random number between 0 and 1 and ΔE is the increment in the energy [21]. The whole procedure is repeated many times for different starting random positions and in this way we are able to obtain both the ground state and the different metastable states.

To study the system at finite temperature, we have followed the MD simulation method [8], referring to the Verlet time integration algorithm [22] and its modified version known as the 'Velocity form' [23, 24] of the Verlet algorithm. In MD simulation, the results of the measurement of a physical quantity (such as temperature or kinetic or potential energy) are obtained as averages of instantaneous values calculated during the MD run. We have performed MD runs up to 5×10^6 steps with a time step size of $\Delta t = 0.001$.

In two-step MD algorithms, as applied in our study, the third order Taylor expansion for the positions $\mathbf{r}$ is written (t) (one forward, one backward in time) [25]. Here the positions $\mathbf{r}$, velocities $\mathbf{v}$ and accelerations $\mathbf{a}$ at time $t + \Delta t$ are obtained from those at time t using the following equations:

$$\mathbf{r}(t + \Delta t) = \mathbf{r}(t) + \mathbf{v}(t)\Delta t + \tfrac{1}{2}\mathbf{a}(t)\Delta t^2$$

$$\mathbf{v}\left(t+\frac{\Delta t}{2}\right)=\mathbf{v}(t)+\frac{1}{2}\mathbf{a}(t)\Delta t$$

$$\mathbf{a}(t+\Delta t)=-\frac{1}{m}\nabla V(\mathbf{r}(t+\Delta t))$$

$$\mathbf{v}(t+\Delta t)=\mathbf{v}\left(t+\frac{\Delta t}{2}\right)+\frac{1}{2}\mathbf{a}(t+\Delta t)\Delta t$$

where Δt is the time step.

As previously [8], starting from the ground state configuration and at $T = 0$, the required temperature of the system T_o was reached in 10^3 MD steps, rescaling the velocities in the expression for $\mathbf{v}(t+\frac{\Delta t}{2})$ so that:

$$\mathbf{v}\left(t+\frac{\Delta t}{2}\right)=\sqrt{\frac{T_o}{T(t)}}\mathbf{v}(t)+\frac{1}{2}\mathbf{a}(t)\Delta t$$

where $T(t)$ is the so-called 'instantaneous temperature'.

Next, in the other 10^3 steps, the system was relaxed. In the final 5×10^6 MD steps the average energies were calculated together with the mean squared displacements.

The loss of order in our 2D Coulomb clusters is investigated through the study of the radial and angular displacement method introduced before [2, 8]. By measuring the mean square displacements (msd) as a function of temperature we can distinguish between the solid and liquid state on the basis of the Lindemann criterion [8]. According to this criterion, if the msd exceed a value of 0.1 then radial or angular melting of the whole system or a given shell appears. We note that in the analysis of Drocco *et al* [5] the mean radial distance of the inner singly charged particles from their initial $T = 0$ position is considered and the melting temperature is defined in a slightly different way. They introduced two melting temperatures: the exchange and rotation temperature and defined the lower one as the melting temperature.

The radial mean square displacement (msd(T)) is defined by

$$\langle u_{\mathrm{R}}^2\rangle=\frac{1}{N_{\mathrm{s}}a^2}\sum_{i=1}^{N_{\mathrm{s}}}[\langle r_i\rangle^2-\langle r_i^2\rangle],$$

where $a=\frac{2R}{\sqrt{N_{\mathrm{s}}}}$ is the average distance between particles, R is the radius of the system and summation is over all particles belonging to a given shell. The symbol $\langle\,\rangle$ stands for an average over the total number of MD steps (after equilibrating the system).

To characterize the angular behavior of the system the intra- and intershell angular mean square deviations can be calculated in order to describe the angular motion of the particles. The angular intrashell square deviation is defined as

$$\langle u_\alpha^2\rangle=\frac{1}{N_{\mathrm{s}}}\sum_{i=1}^{N_{\mathrm{s}}}[\langle(\varphi_i-\varphi_{i_1})^2\rangle-\langle\varphi_i-\varphi_{i_1}\rangle^2]/(\varphi_o^{(s)})^2$$

and the angular intershell square deviation is defined as

$$\langle u_\beta^2\rangle=\frac{1}{N_{\mathrm{s}}}\sum_{i=1}^{N_{\mathrm{s}}}[\langle(\varphi_i-\varphi_{i_2})^2\rangle-\langle\varphi_i-\varphi_{i_2}\rangle^2]/(\varphi_o^{(s)})^2$$

where i_1 is the nearest particle from the same shell, i_2 is the nearest particle from the nearest neighbor shell, $\varphi_o=\frac{2\pi}{N_{\mathrm{s}}}$ and N_{s} is the number of particles in a shell.

3. Results

We have investigated systems consisting of $N = 10$ particles as a function of the parameter $q = 0.1, 0.4, 0.8, 1, 1.5, 2, 3, 5$. The ground state configurations of non-equally charged particles have been found by using the MC algorithm of Bedanov *et al* [2] and Kong *et al* [9]. The particles arrange themselves in concentric rings as seen in figure 1. The black filled circles correspond to particles with charge $q_1 = 1$ and the open red circles to those with charge $q_2 = q$. The particles carrying larger charge are pushed to peripheral rings to minimize the repulsion, which agrees with previous observations [5, 12].

However, we see that the ring structure changes with q. The structural data on the configuration for the ground and for the metastable states are presented in table 1 for different values of q. For $q \neq 1$ we found that the outer ring always has five particles, both for the ground state and all metastable states. The values of energy per particle E/N and also the differences in energy between the metastable state and the ground state $\Delta E/N$ are given. Notice that the number of metastable states depends sensitively on q.

For $q = 1$ we recover the known structure [9] (2, 8), but for $q \geqslant 2$ or $q \leqslant 0.4$, we find (5, 5) partitioning, which is consistent with that in figures 1(a)–(d) and 2(a) of Ferreira *et al* [12]. In this case, there is a clear separation in shells between the two types of particles. We can also distinguish the (3, 7) and (3, 2, 5) structures, as far as intermediate values of q are concerned. For $q = 0.8$ and 1.5 we have three rings. With increasing q, the radius of the rings increases.

The region near $q = 1$ was considered in [12] for $N = 10$ and 13. In this case (figures 2 and 3 in [12]) a structural discontinuity was observed. In figure 3 in [12] a structural phase transition can be distinguished for $q = 1$, as there are discontinuities in the derivatives of the energy with respect to q. Here we analyze only the melting for $q = 1$ and q much different from 1.

For different q the rings have different widths (given in table 1). In figure 2 we present the q dependent widths of rings for the ground states. For $q \leqslant 0.4$ and $q \geqslant 3.0$ there are perfect rings (both inner and outer ones) and we can observe magic configurations (5, 5). For metastable states we can distinguish mostly the (3, 2, 5) structures in the range of q $0.8 \leqslant q \leqslant 2.0$ except $q = 1$, and for $q < 0.8$ or $q > 2.0$ we found the configuration with one particle in the middle (1, 4, 5), (1, 3, 1, 5).

The results for melting properties of our system are summarized in figures 3 and 4. We took the following convention: T_{R} indicates radial melting temperature and T_α and T_β indicate the angular intrashell and intershell melting temperatures, respectively. They represent the temperatures at which the msd $\langle u_{\mathrm{R}}^2\rangle$, $\langle u_\alpha^2\rangle$ and $\langle u_\beta^2\rangle$ exceed the value of 0.1. In order to simplify the plots in the case of $q = 0.8$ and 1.5, $T_{\mathrm{R}1}$ and $T_{\alpha 1}$ describe the melting temperatures of the inner two rings for which those values are the same (see also table 2).

Table 2 summarizes the results shown in figures 2 and 3 and presents a sequence of melting steps for different q s. In addition in table 3 we present for a specific q-value, i.e. $q = 3$,

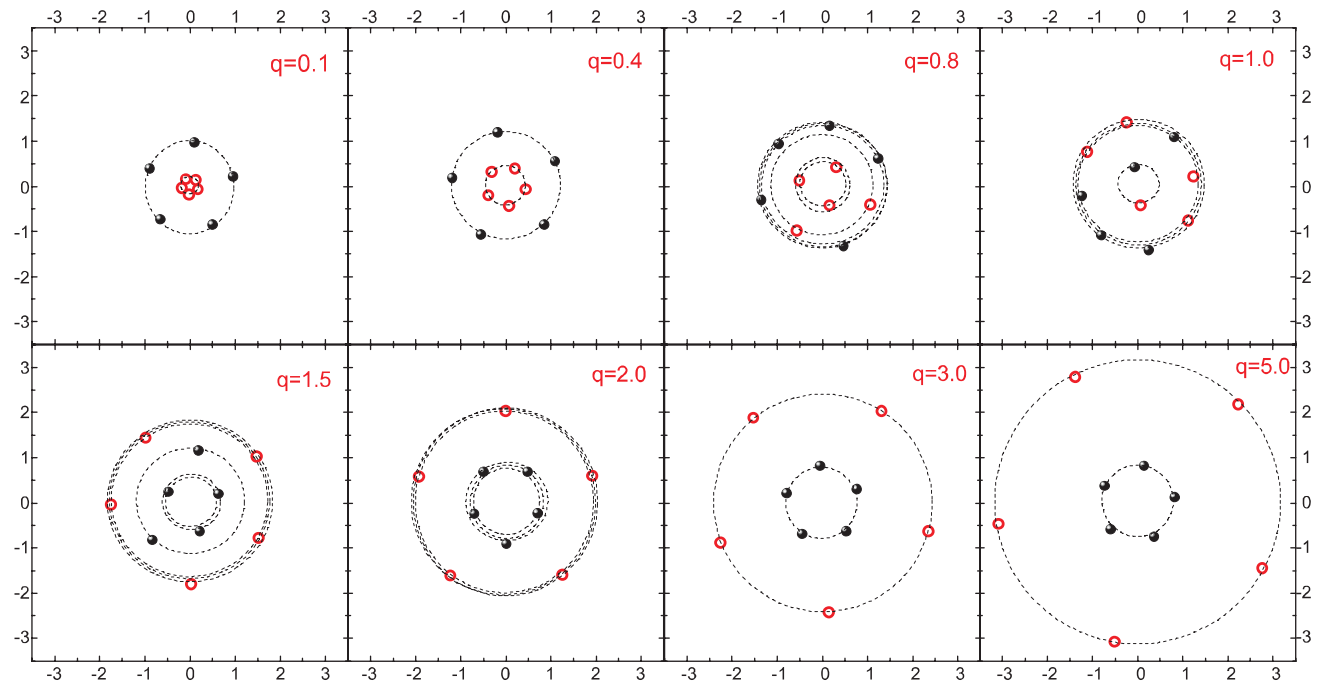

Figure 1. Ground state configurations of the 10-particle system for $q = 0.1, 0.4, 0.8, 1, 1.5, 2, 3, 5$. The filled circles represent particles with charge equal to 1 and the open circles denote the particles with different charge q.

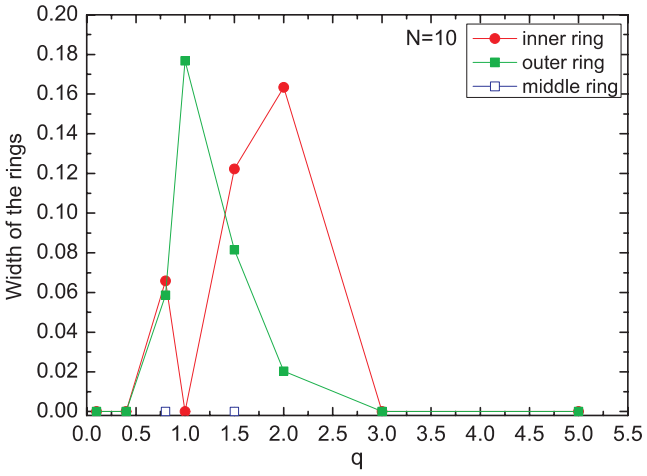

Figure 2. Width of the rings versus q for the ground state. The widths are marked as follows: filled red circles refer to the width of the inner ring, filled green squares refer to width of the outer ring, and blue open squares refer to width of the middle ring.

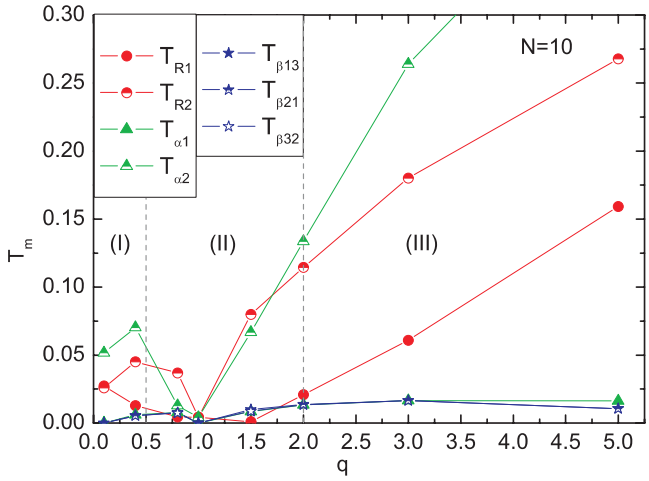

Figure 3. Radial and angular intrashell melting temperatures (according to the Lindemann criterion) of both rings versus the ratio q between the charges. The temperatures are marked as follows: filled red circles (T_{R_1}) represent radial displacements for the inner rings; half-filled red circles (T_{R_2}) represent radial displacements for the outer ring; filled green triangles ($T_{\alpha 1}$) are angular intrashell displacements for the inner rings; half-filled green triangles ($T_{\alpha 2}$) are angular intrashell displacements for the outer ring; and blue stars are angular intershell displacements (T_β).

the numerical values for the different radial and angular intra- and intershell variations for different temperatures. The bold results are for those were melting occurs.

Figure 3 presents the radial, intra- and intershell melting temperatures of the rings for $q = 0.1$–5.0. In figure 4 we present the angular intershell temperatures and angular intrashell temperatures of inner rings in more detail.

Except for $q = 0.8$ and 1.5, first intershell rotation occurs and melting of the system is accomplished with intrashell melting of the outer ring. For $q = 0.8$ and 1.5 first the radial melting of both inner rings is observed. Similar behavior was found previously by Drocco *et al* [5] where for the configuration (1, 6, 6) the melting temperature is that at which radial exchange of particles between shells is observed while rotation does not yet occur (see figure 6(b) in [5]). Another reason for the different scenario might be the broadening of one of the two inner rings and the fact that in both cases the two inner rings consist of particles with the same type of

Table 1. The ground state and metastable states for Coulomb clusters consisting of $N = 10$ particles and with varying charge ratio $q = q_1/q_2 = 0.1$–5.0; the columns contain energy E/N, $\Delta E/N$, shell structure, radius and width of the rings. The energy is in units of E_o and coordinates are in units of r_o.

q	E/N	$\Delta E/N$ ($E_{\text{metastable}} - E_{\text{groundstate}})/N$	Configuration	Radius of the ring	Width of the ring
0.1	1.494 12	—	5, 5	0.981 22	0
				0.182 44	0
	1.494 82	0.0007	1, 4, 5	0.001 03	0
				0.204 83	0.000 32
				0.981 32	0.000 92
0.4	2.501 07	—	5, 5	0.444 25	0
				1.212 45	0
0.8	3.834 45	—	3, 2, 5	0.498 22	0.065 82
				1.134 12	0
				1.375 42	0.058 67
	3.835 07	0.000 62	3, 2, 5	0.499 89	0.020 44
				1.125 43	0
				1.377 98	0.096 68
	3.837 65	0.003 20	3, 2, 5	0.496 24	0.077 51
				1.177 45	0.125 64
				1.361 25	0.082 46
	3.867 45	0.033 00	3, 2, 5	0.526 11	0.117 59
				1.154 76	0.067 94
				1.368 28	0.183 45
	3.871 18	0.036 73	3, 2, 5	0.519 83	0.029 33
				1.186 77	0.094 24
				1.361 53	0.061 66
	3.906 18	0.071 73	2, 3, 5	0.458 73	0.194 49
				1.079 45	0.164 63
				1.342 88	0.237 18
1.0	4.484 94	—	2, 8	0.426 49	0
				1.348 79	0.176 77
	4.488 16	0.003 22	3, 7	0.567 73	0.053 11
				1.412 93	0.140 64
1.5	5.831 16	—	3, 2, 5	0.623 66	0.122 35
				1.172 55	0
				1.761 01	0.081 54
	5.833 43	0.002 27	3, 2, 5	0.587 68	0.154 27
				1.264 44	0
				1.743 08	0.080 65
	5.842 85	0.011 69	3, 2, 5	0.601 45	0.113 74
				1.288 20	0.301 62
				1.732 80	0.090 38
2.0	7.151 79	—	5, 5	0.817 60	0.163 50
				2.023 69	0.020 37
	7.166 21	0.014 42	1, 3, 1, 5	0.275 80	0
				0.837 31	0.203 19
				1.212 71	0
				2.012 42	0.032 23
3.0	9.850 15	—	5, 5	0.820 30	0
				2.427 73	0
5.0	15.632 69	—	5, 5	0.830 00	0
				3.119 76	0
	15.650 14	0.017 45	1, 4, 5	0.023 65	0
				0.928 99	0.006 36
				3.121 36	0.009 79

charge. Moreover, for $q = 0.8$ and 1.5 the shell configurations are similar (3, 2, 5). Having this in mind, we have done calculations for three separate rings in those two cases, and we noted that in both cases at first there is radial melting of the inner rings, next angular inter- and intrashell melting of rings 1 and 2 and everything is followed by angular intrashell and later also radial melting of ring number 3.

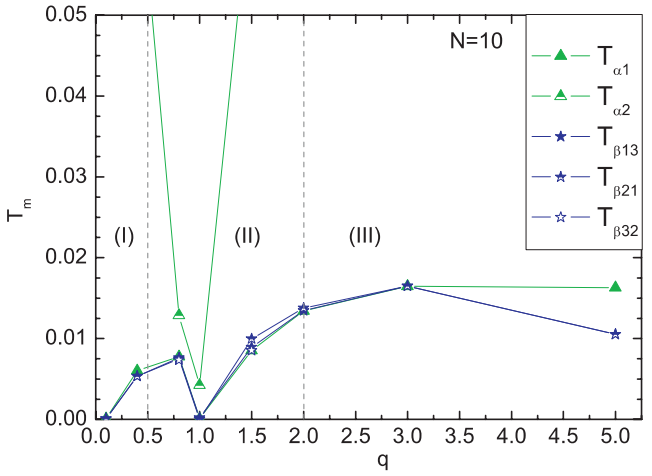

Figure 4. Angular intrashell and intershell melting temperatures (according to the Lindemann criterion) of both rings versus the ratio q of the charges. The temperatures are marked as follows: filled green triangles ($T_{\alpha 1}$) refer to angular intrashell displacements for the inner rings; half-filled green triangles ($T_{\alpha 2}$) refer to angular intrashell displacements for the outer ring; blue stars are angular intershell displacements (T_β).

Following the work of Ferreira *et al* [12] we have concentrated on melting properties in specific q intervals, with characteristic ground state symmetries. The presence of perfect ring-like structures and magic configurations (5, 5) in regions I and III has been confirmed (figures 1(a)–(d) and 2(a) in [12]). The sequences of melting steps are presented in table 2.

For $q = 0.1$ the sequence is as follows: $0 = T_\beta = T_{\alpha 1} < T_{\mathrm{R}1} = T_{\mathrm{R}2} < T_{\alpha 2}$. The rotations and angular intrashell melting of the inner ring appear at any finite temperature. They are followed by the radial melting of the rings, and the melting process is completed with angular intrashell fluctuations of the outer ring.

Excluding the cases of $q = 0.1$ and 1.0, we observe a clear angular intershell melting temperature.

For the value $q = 0.4$, which belongs to region I, the rotation occurs at a finite temperature, $0 < T_\beta = T_{\alpha 1} < T_{\mathrm{R}1} < T_{\mathrm{R}2} < T_{\alpha 2}$. For $q = 2.0$ and 3.0 (referring to region III in Ferreira *et al*'s work [12]), first the angular intrashell melting of the inner ring occurs together with intershell rotation, then the inner ring melts radially, which is followed by radial melting of the outer ring, and finally the outer ring loses the inner angular order. The case $q = 5.0$ differs in the fact that rotation is earlier than angular disorder of the inner ring. We can confirm that region III is very similar to region I in the sense that first rotations occur at the same temperature (or at a very similar temperature for case of $q = 5.0$) as that at which the inner ring loses angular order, and than one ring after another undergoes radial melting and the whole process is accomplished with the loss of angular order in the outer ring.

Table 2. The q-dependent sequence of melting steps. $T_{\mathrm{R}x}$ and $T_{\alpha x}$ are the radial and intrashell melting temperatures, respectively, x is the ring number, where numbering starts from the center, and $T_{\beta xy}$ is the intershell melting temperature of ring x with respect to ring y, where $T_{\beta xy} = T_{\beta yx}$.)

q	No. of rings	Step no. 1	Step no. 2	Step no. 3	Step no. 4
0.1	2	$0 = T_{\beta 21} = T_{\alpha 1}$	$T_{\mathrm{R}1} \approx T_{\mathrm{R}2}$	$T_{\alpha 2}$	—
0.4	2	$T_{\beta 21} = T_{\alpha 1}$	$T_{\mathrm{R}1}$	$T_{\mathrm{R}2}$	$T_{\alpha 2}$
0.8	3	$T_{\mathrm{R}1} = T_{\mathrm{R}2}$	$T_{\alpha 1} = T_{\alpha 2} = T_{\beta 13} = T_{\beta 21} = T_{\beta 32}$	$T_{\alpha 3}$	$T_{\mathrm{R}3}$
1.0	2	$0 = T_{\beta 12} = T_{\alpha 1}$	$T_{\mathrm{R}1} = T_{\mathrm{R}2} = T_{\alpha 2}$	—	—
1.5	3	$T_{\mathrm{R}1} = T_{\mathrm{R}2}$	$T_{\alpha 1} = T_{\alpha 2} = T_{\beta 13} = T_{\beta 21} = T_{\beta 32}$	$T_{\alpha 3}$	$T_{\mathrm{R}3}$
2.0	2	$T_{\beta 21} = T_{\alpha 1}$	$T_{\mathrm{R}1}$	$T_{\mathrm{R}2}$	$T_{\alpha 2}$
3.0	2	$T_{\beta 21} = T_{\alpha 1}$	$T_{\mathrm{R}1}$	$T_{\mathrm{R}2}$	$T_{\alpha 2}$
5.0	2	$T_{\beta 21} < T_{\alpha 1}$	$T_{\mathrm{R}1}$	$T_{\mathrm{R}2}$	$T_{\alpha 2}$

Table 3. A sample of our results for $q = 3.0$ in order to illustrate in more detail the sequence of melting steps for the ground state. The radial $\langle u^2_{\mathrm{R}x}\rangle$, intrashell $\langle u^2_{\alpha x}\rangle$ (x is the ring number, $x = 1$ for the inner ring, $x = 2$ for the outer one) and intershell $\langle u^2_{\beta 21}\rangle$ displacements are presented for appropriate temperatures at which melting can be observed. T_{m} is the melting temperature according to the Lindemann criterion. The considered temperatures were chosen to be larger than the melting temperatures in order to ensure that the system was clearly in the melted state.

$T \gtrsim T_{\mathrm{m}}$	$\langle u^2_{\mathrm{R}1}\rangle$	$\langle u^2_{\mathrm{R}2}\rangle$	$\langle u^2_{\alpha 1}\rangle$	$\langle u^2_{\alpha 2}\rangle$	$\langle u^2_{\beta 21}\rangle$
0.035	0.056	0.018	**2.436**	0.006	**1.996**
0.066	**0.108**	0.033	2.542	0.010	2.064
0.264	0.249	**0.139**	2.493	0.040	2.107
0.355	0.305	0.189	2.473	**0.452**	2.130

Region II contains interesting cases of $q = 0.8, 1.0, 1.5$. Note that $q = 1.0$ is a specific case where we recognize two-step melting (as previously found in [8] for varying numbers of particles N): at first the angular intrashell melting of the inner ring and rotation occur and afterward radial melting of both rings together with angular intrashell melting of the outer ring. There is very low intershell rotation locking, resulting in a reduced melting temperature (T_β), while we would expect this to be larger in case of a magic configuration—it seems to be of a similar order of magnitude to that for nine particles (which is not a magic configuration). The reason for the specific scenario in this case is not known to us.

But, $q = 1.0$ and 0.1 are particular exceptions (among the investigated uniformly and non-uniformly charged particles) in that at first around $T = 0$ the inner ring loses its angular order (directly $T_{\alpha 1}$ is greater than 0.1). From symmetry, we can expect that in the case of $q \approx 10.0$ we will find rotation at $T = 0$. The radial order of the rings is preserved together with the angular intrashell order of the outer ring until the system melts completely. The shell structure of $N = 9$ (2, 7) and 10 (2, 8) differs in the fact that for $N = 9$ two central particles have different radial positions while for $N = 10$ they have the same positions.

For q significantly different from 1, a new behavior is found. Although intershell rotation occurs for T just above $T = 0$, as for the uniform system, and the inner ring loses angular intrashell order, the radial order of the rings is preserved together with the angular intrashell order of the outer ring. Increasing the temperature, first the inner shell becomes unstable due to strong radial displacements, which is demonstrated by the filled circles in figure 3. Afterward the outer shell becomes smeared out as shown by the half-filled circles, and finally the diffusion between shells destroys the radial order. The melting process is completed when the intrashell angular displacements of the outer ring overcome a threshold (the upper curve denoted by the triangles in figure 4). This four-step scenario is different from that in the uniform limit [8] and is consistent with the findings of Drocco *et al* [5], who defined two characteristic temperatures for the angular and radial behavior; these were found to be different from each other and the melting temperature was assumed to correspond to the lower one in figure 3.

In all the cases intershell rotation is accomplished very quickly, mostly with the loss of angular inner shell order of the inner ring (figure 4) which is a q-independent feature.

Ferreira *et al* [19] were considering melting of the inner ring for the case of $N_f = 7, N_v = 6, q = 3.0$;: first they found intershell rotation around 0.01, then angular intrashell melting and radial melting at a similar temperature $T = 0.02$–0.025. For our case $N_f = 5, N_v = 5, q = 3.0$ we observe intershell rotation around $T = 0.017$, which is similar. But we observed a different behavior: for the inner ring we have angular intrashell and intershell melting almost together at $T = 0.013$, and radial melting of the inner ring at a much higher temperature $T = 0.06$.

For the magic configuration (5, 5) there is rotation at finite temperature, what is consistent with our previous work [8]. This is no longer the case for very large and very small q and $q = 1.0$. For $q = 0.1$, 1.0, and $q > 5.0$ intershell rotation occurs for $T \approx 0$, due to the large difference in radii of the rings.

4. Summary and conclusions

In conclusion, using the Monte Carlo algorithm of [2, 9], we have determined the ground state and metastable configurations which depend on q. Following our previous MD approach we found a new dependence of the melting temperature on the q ratio for small confined clusters of charged particles [8].

Starting from the ground state configurations, we found several interesting melting behaviors in the vicinity of $q = 1.0$ and for q significantly different from 1: the four-step melting behavior, which for q significantly different from 1 starts from the intershell rotation accompanied by the intrashell angular

disorder of the inner ring, followed by radial melting of the inner ring, and next radial melting of the outer ring, completed with the intrashell angular disorder of the outer ring. For q-values near $q = 1.0$ (for $q = 0.8$ and 1.5) we found another scenario, due to the three ring configurations, in which at first there is radial melting of the two inner rings, next angular inter- and intrashell melting of those rings and everything is followed by angular intrashell and later also radial melting of the outer ring.

Acknowledgments

This work was partially supported by the Polish Ministry of Science and Education via the grant 4 T11F 014 24, the European Community within the MAGMANet project NMP3-CT-2005-515767, and the Flemish Science Foundation (FWO-Vl).

References

[1] Juan W T, Huang Z H, Hus J W, Lai Y J and I L 1998 *Phys. Rev.* E **58** 6947
[2] Bedanov V M and Peeters F M 1994 *Phys. Rev.* B **49** 2667
[3] Schweigert V A and Peeters F M 1995 *Phys. Rev.* B **51** 7700
[4] Schweigert I V, Schweigert V A and Peeters F M 1996 *Phys. Rev.* B **54** 10827
[5] Drocco J A, Olson Reichhardt C J, Reichhardt C and Janko B 2003 *Phys. Rev.* E **68** 060401
[6] Kamieniarz G and Sobczak P 2008 *Acta Phys. Pol.* A **113** 477–80
[7] Munarin F F, Nelissen K, Ferreira W P, Farias G A and Peeters F M 2005 *Phys. Rev.* E **72** 021406
[8] Tomecka D M, Partoens B and Peeters F M 2005 *Phys. Rev.* E **71** 062401
[9] Kong M, Partoens B and Peeters F M 2002 *Phys. Rev.* E **65** 046602
[10] Egger R, Haüsler W, Mak C H and Grabert H 1999 *Phys. Rev. Lett.* **82** 3320
[11] Filinov A V, Bonitz M and Lozovik Yu E 2001 *Phys. Rev. Lett.* **86** 3851
[12] Ferreira W P, Munarin F F, Nelissen K, Costa Filho R N, Peeters F M and Farias G A 2005 *Phys. Rev.* E **72** 021406
[13] de Moraes S S, Coimbra D, de Sousa J R and da Frota H O 2004 *Braz. J. Phys.* **34** 2A
[14] Castelano L K, Hai G-Q, Partoens B and Peeters F M 2006 *Phys. Rev.* B **74** 045313
[15] Thomson J J 1904 *Phil. Mag.* **7** 237
[16] Saint Jean M, Even C and Guthmann C 2001 *Europhys. Lett.* **55** 45
[17] Nelissen K, Partoens B and Peeters F M 2004 *Phys. Rev.* B **69** 046605
[18] Nelissen K, Partoens B, Schweigert I and Peeters F M 2006 *Europhys. Lett.* **74** 1046
[19] Ferreira W P, Munarin F F, Farias G A and Peeters F M 2006 *J. Phys.: Condens. Matter* **18** 9385
[20] Metropolis N, Rosenbluth A W, Rosenbluth M N, Teller A M and Teller E 1953 *J. Chem. Phys.* **21** 1087
[21] Schweigert I V, Schweigert V A and Peeters F M 1999 *Phys. Rev. Lett.* **82** 5293
[22] Verlet L 1967 *Phys. Rev.* **159** 98
Verlet L 1967 *Phys. Rev.* **165** 201
[23] Swope W C, Andersen H C, Berens P H and Wilson K R 1982 *J. Chem. Phys.* **76** 637
[24] Rapaport D C 1995 *The Art of Molecular Dynamics Simulation* (Cambridge: Cambridge University Press)
[25] Ercolessi F 1997 *A Molecular Dynamics Primer* International School for Advanced Studies (SISSA-ISAS), Spring College in Computational Physics, ICTP, Trieste